VIBRATION CONTROL AND CALCULATING INVERSE DYNAMICS OF THE RIGID-FLEXIBLE TWO-LINK MANIPULATOR T-R

Nguyen Van Khang[1,*] , **Dinh Cong Dat**[1,2]
[1]*Hanoi University of Science and Technology, Vietnam*
[2]*Hanoi University of Mining and Geology, Vietnam*
[*]E-mail: khang.nguyenvan2@hust.edu.vn

Abstract. Research on the dynamics and control of flexible link manipulators (FLMs) is increasing in the industrial robotics, but the problem of inverse dynamics of the flexible link manipulators has been paid a little attention. In this paper, an approximation method is presented to calculate the reverse dynamics of the serial manipulators with rigid-flexible links. The linearization of the motion equations for a rigid-flexible translation and rotation of two-link manipulator (manipulator T-R) is addressed. The vibration control and calculating inverse dynamics of a periodic rigid-flexible two-link manipulator T-R are studied. The Taguchi method is used for the design of gain values of the controller PD for the manipulator. The results of numerical simulation show the efficiency and usefulness of the proposed method.

Keywords: flexible manipulator, linearization, Floquet theory, vibration control, Taguchi method, inverse dynamics.

1. INTRODUCTION

The modeling and control of flexible manipulators are increasing in industrial robotics research. Recent valuable reviews on dynamics and control of flexible robots related to the existing works till 2016 are provided in some articles [1–4]. According to these works, the stability and vibration analysis of flexible robots have been little studied. It should be noted that in many applications of robot design and control, the computation of the full flexible model of a robot is not necessary, while the knowledge of its natural frequencies is required.

The forward dynamics problems of flexible manipulators have been considered in articles [5–10]. In which force/moments of the joint links are known quantities, and motions of the joint links are the quantities to be found. In [11–15], the inverse dynamics of flexible manipulators have been studied in the problems of set-point regulation.

In general terms, an inverse dynamic problem for a serial manipulator is the problem of finding the joint torques that will produce a given motion of the end-effector. The inverse dynamics is originally designed to control the robotic manipulator. If the desired motion of the rigid manipulator is chosen as the fundamental motion, the equation for the error dynamics of a flexible manipulator in the first order approximation has the same form as [16–18]

$$\dot{\mathbf{x}} = \mathbf{A}(t)\mathbf{x} + \mathbf{f}(t).$$

Motion control problems of flexible manipulators can be divided into two classes: regulation and tracking control. The regulation is the control problem around the desired equilibrium configuration of manipulators, in which the regulation $\mathbf{q}_d$ is constant and $\dot{\mathbf{q}}_d = \ddot{\mathbf{q}}_d = \mathbf{0}$. If the equilibrium configuration of a rigid manipulator is chosen as the fundamental motion, the matrix $\mathbf{A}$ is a constant matrix. If the desired motion of the joint coordinates $\mathbf{q}_d(t)$, velocity $\dot{\mathbf{q}}_d(t)$, and acceleration $\ddot{\mathbf{q}}_d(t)$ are periodic function, the matrix $\mathbf{A}(t)$ is a periodic matrix.

Robots with flexible links are vibration systems. Therefore, the most important problem in robots with flexible links is the problem of determining the natural frequencies (when $\mathbf{A}$ is a constant matrix) or the dynamic stability domain (when $\mathbf{A}(t)$ is a periodic matrix). When studying the dynamics of a multi-body system with flexible links [19], Briot and Khalil have written: "In many applications of robot design and control, the computation of the full electrodynamic model of a robot is not necessary, while the knowledge of its natural frequencies is required". We completely agree with this thinking. It can be said that the above thinking is the basic idea of this paper.

For the serial manipulator with rigid links, if the end-effector motion is known, inverse dynamics allows computation of the joint torques to the joints to obtain the desired motion of the end-effector. For the serial manipulator with flexible links, if the end-effector motion is known, we can not calculate the desired motion of the end-effector. Because we don't know the motion of the elastic coordinates. The inverse dynamics analysis for flexible robots by tracking control has been little studied, and the dynamic stability control of flexible manipulators is presently still an open problem. Robots with elastic links are vibration systems. Therefore, the most important problem in robots with flexible links is the problem of determining the natural frequencies, if the matrix $\mathbf{A}$ is a

constant matrix or determining the dynamic stability domain if the matrix $\mathbf{A}(t)$ is a periodic matrix. The main contribution of this paper is the study of dynamic stability control and the calculation of periodic vibration of a rigid-flexible two-link manipulator. Then it is possible to calculate the approximate force/torque of the actuators of the rigid-flexible two-link manipulator T-R.

2. LINEARIZATION OF THE MOTION EQUATIONS ABOUT THE FUNDAMENTAL MOTION

Let us consider now the vertical-planar motion of a rigid-flexible two-link translation and rotation manipulator (manipulator T-R) shown in Fig. 1, where the rigid link OB (link 1) is assumed to be uniform. The link DE (link 2) in Fig. 1(a) is rigid link. The link DE (link 2) in Fig. 1(b) is flexible link. The flexible link DE in Fig. 1(b) is clamped to the rigid moving base and assumed to be thin, uniform, and satisfies the Euler–Bernoulli beam assumptions of small shear and rotary inertia effects. Both links are connected by disc B which moves on the plane. The payload mass at the free end of link 2 can move without friction relative to the link using a force actuator. Using the floating frame of reference approach [1], the motion equations of some two-link rigid-flexible manipulators are derived in reference [20].
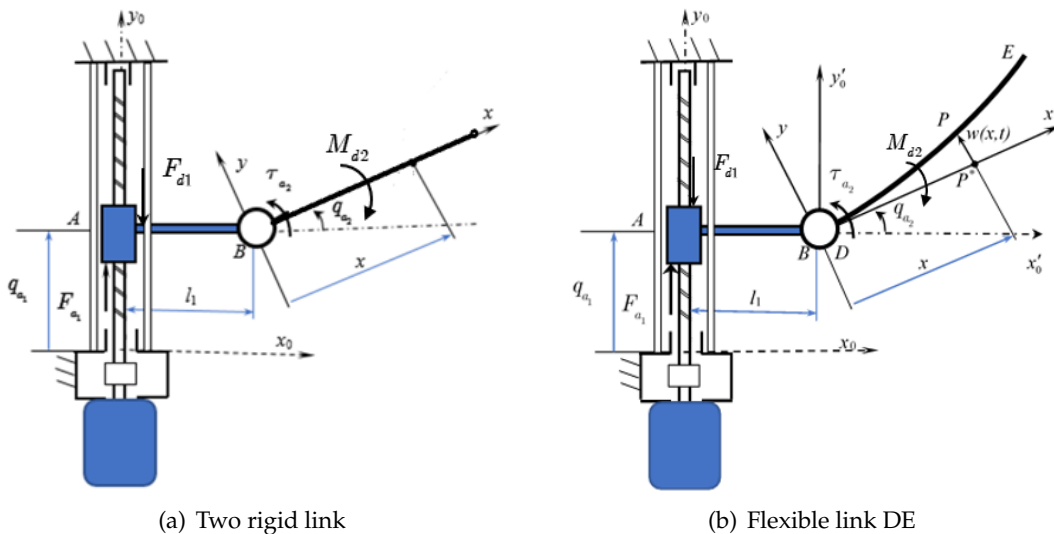

(a) Two rigid link   (b) Flexible link DE

Fig. 1. Manipulator T-R

In this section, we focus on the linearization of motion equations of flexible manipulator based on inverse dynamics of the virtual rigid motion of flexible link which is given

in [20]. The differential equations of motion of the two-link rigid-flexible manipulator can be expressed in the compact matrix form [15, 18]

$$\mathbf{M}(\mathbf{q})\ddot{\mathbf{q}} + \mathbf{C}(\mathbf{q}, \dot{\mathbf{q}})\dot{\mathbf{q}} + \mathbf{g}(\mathbf{q}) = \boldsymbol{\tau}(t), \tag{1}$$

where $\mathbf{q}, \dot{\mathbf{q}}$ and $\ddot{\mathbf{q}}$ are the generalized coordinates, velocities, and accelerations, respectively. For simplicity, we choose an elastically generalized coordinate and denote it by q_e. The generalized coordinates, velocities, and accelerations of the rigid-flexible two-link manipulator T-R have the following form [20]

$$\mathbf{q} = [q_{a1}, q_{a2}, q_e]^T, \quad \boldsymbol{\tau}(t) = [\tau_{a1}(t), \tau_{a2}(t), \tau_e(t)]^T = [\tau_{a1}(t), \tau_{a2}(t), 0]^T. \tag{2}$$

Let $\Delta q_{a1}, \Delta q_{a2}$ and Δq_e are the difference between the real motion $\mathbf{q}(t)$ and the fundamental motion $\mathbf{q}^R(t)$, we have

$$y_1(t) = \Delta q_{a1} = q_{a1}(t) - q_{a1}^R(t), \ y_2(t) = \Delta q_{a2} = q_{a2}(t) - q_{a2}^R(t), \ y_3(t) = \Delta q_e = q_e(t), \tag{3}$$

where y_1, y_2 and y_3 are called the perturbed motion. Similarly, it follows that

$$\boldsymbol{\tau}(t) = [\tau_{a1}(t), \tau_{a2}(t), \tau_e(t)]^T = [\tau_{a1}(t), \tau_{a2}(t), 0]^T. \tag{4}$$

The elements $q_{a1}^R(t), q_{a2}^R(t)$ are given in [20].

By substituting Eqs. (3) into Eq. (1) and using Taylor series expansion around fundamental motion [20–22], then neglecting nonlinear terms, we obtain the system of linear differential equations with time-varying coefficients for the single-link flexible manipulator as follows

$$\mathbf{M}_L(t)\ddot{\mathbf{y}} + \mathbf{C}_L(t)\dot{\mathbf{y}} + \mathbf{K}_L(t)\mathbf{y} = \mathbf{h}_L(t). \tag{5}$$

The matrices $\mathbf{M}_L(t), \mathbf{C}_L(t), \mathbf{K}_L(t)$ and vector $\mathbf{h}_L(t)$ of the linear differential equations according to Eq. (5) have the following forms

$$\mathbf{M}_L(t) = \begin{bmatrix} (m_1 + m_2 + m_B) & \left(\frac{1}{2}m_2 l_2 + m_2 r\right)\cos q_{a2}^R & \mu C_1 \cos q_{a2}^R \\ \left(\frac{1}{2}m_2 l_2 + m_2 r\right)\cos q_{a2}^R & J_B + m_2 r^2 + m_2 r l_2 + \frac{1}{3}m_2 l_2^2 & \mu r C_1 + \mu D_1 \\ \mu C_1 \cos q_{a2}^R & \mu r C_1 + \mu D_1 & \mu n_{11} \end{bmatrix}, \tag{6}$$

$$\mathbf{C}_L(t) = \begin{bmatrix} 0 & -(m_2 l_2 + 2m_2 r)\dot{q}_{a2}^R \sin q_{a2}^R & -2\mu C_1 \dot{q}_{a2}^R \sin q_{a2}^R \\ 0 & 0 & 0 \\ 0 & 0 & 0 \end{bmatrix}, \tag{7}$$

$$\mathbf{K}_L(t) = \begin{bmatrix} 0 & -\left(\frac{m_2 l_2}{2} + m_2 r\right)\left[\ddot{q}_{a2}^R \sin q_{a2}^R + \left(\dot{q}_{a2}^R\right)^2 \cos q_{a2}^R\right] & -\mu C_1 \left[\ddot{q}_{a2}^R \sin q_{a2}^R + \left(\dot{q}_{a2}^R\right)^2 \cos q_{a2}^R\right] \\ 0 & -\left(\frac{1}{2}m_2 l_2 + m_2 r\right)\left(\ddot{q}_{a1}^R + g\right)\sin q_{a2}^R & -\mu C_1 \left(\ddot{q}_{a1}^R + g\right)\sin q_{a2}^R \\ 0 & -\mu C_1 \left(\ddot{q}_{a1}^R + g\right)\sin q_{a2}^R & EI k_{11}^* - \mu \left(\dot{q}_{a2}^R\right)^2 n_{11} \end{bmatrix}, \tag{8}$$

$$\mathbf{h}_L(t) = \begin{bmatrix} 0 \\ 0 \\ -\mu g C_1 \cos q_{a2}^R - \mu C_1 \ddot{q}_{a1}^R \cos q_{a2}^R - (\mu r C_1 + \mu D_1) \ddot{q}_{a2}^R \end{bmatrix}. \tag{9}$$

Table 1. Parameters of the manipulator

Parameters of the model	Variable and unit	Value
Length of link 1	$l_1 \, (\mathrm{m})$	0.1
Mass of link 1	$m_1 \, (\mathrm{kg})$	1.32
Mass of disc B	$m_B \, (\mathrm{kg})$	0.1
Radius of disc B	$r \, (\mathrm{m})$	0.02
Mass moment of inertia of disc B	$J_B \, (\mathrm{kg \, m^2})$	4.5×10^{-5}
Length of link 2	$l_2 \, (\mathrm{m})$	0.3
Cross-sectional area of link 2	$A \, (\mathrm{m^2})$	2×10^{-5}
Density of link 2	$\rho \, (\mathrm{kg/m^3})$	7850
Modulus of link 2	$E \, (\mathrm{N/m^2})$	7.11×10^{10}
Inertial moment of sectional area of link 2	$I \, (\mathrm{m^4})$	1.67×10^{-12}
Drag coefficient	$\alpha_1 \, (\mathrm{N \, m \, s/rad})$	0.02
Drag coefficient	$\alpha_2 \, (\mathrm{N \, m \, s/rad})$	0.01

For numerical simulation, the parameters of the considered flexible manipulator are listed in Table 1. From the parameters in Table 1, we have

$$\begin{aligned} C_1 &= -0.2348772632, \ D_1 = -0.0511900094, \\ n_{11} &= 0.2999500508, \ k_{11}^* = 457.7890772, \ X_1 = -1.999847202. \end{aligned} \tag{10}$$

3. DYNAMIC STABILITY CONTROL OF THE FLEXIBLE MANIPULATOR T-R USING THE FLOQUET THEORY

3.1. Calculating Floquet multipliers of linear differential systems with time-periodic coefficients

In the steady of a flexible manipulator, the matrices $\mathbf{M}_L(t), \mathbf{C}_L(t), \mathbf{K}_L(t)$ and vector $\mathbf{h}_L(t)$ of the linear differential equations (5) are time-periodic with the least period $T = 2\pi/\Omega$. For calculation of dynamic stability condition, we shall consider a system of homogeneous linear differential equations

$$\mathbf{M}_L(t)\ddot{\mathbf{y}} + \mathbf{C}_L(t)\dot{\mathbf{y}} + \mathbf{K}_L(t)\mathbf{y} = 0. \tag{11}$$

According to Floquet theory [16,17], the characteristic equation of Eq. (11) is independent of the chosen fundamental set of solutions. From the parameters of the manipulator given in Table 1, we can determine the Floquet multipliers $\rho_k (k = 1, \ldots, n)$ of the system of differential equations (11) according to the algorithm presented in the document [23]. If $|\rho_k| < 1$, the trivial solution $\mathbf{y} = 0$ of Eq. (11) will be asymptotically stable. Conversely, the solution $\mathbf{y} = 0$ of Eq. (11) becommes unstable if at least one Floquet multiplier has modulus being larger than 1. In this case, we need to design the controller for stabilising the motion of the flexible manipulator. Some calculation results of the maximum value of the Floquet multipliers are listed in Table 2.

Table 2. Modulus of Floquet multipliers for four cases

Case 1: $\Omega = \pi$	$\|\rho_1\| = 1$, $\|\rho_2\| = 22.6578$, $\|\rho_3\| = 0.1304$, $\|\rho_4\| = 0.9293$, $\|\rho_5\| = 0.9293$, $\|\rho_6\| = 0.9729$
Case 2: $\Omega = 2\pi$	$\|\rho_1\| = 1$, $\|\rho_2\| = 10.8771$, $\|\rho_3\| = 0.9864$, $\|\rho_4\| = 0.0893$, $\|\rho_5\| = 0.9844$, $\|\rho_6\| = 0.9844$
Case 3: $\Omega = 4\pi$	$\|\rho_1\| = 1$, $\|\rho_2\| = 0.9935$, $\|\rho_3\| = 0.9935$, $\|\rho_4\| = 0.9934$, $\|\rho_5\| = 0.9934$, $\|\rho_6\| = 0.9934$
Case 4: $\Omega = 8\pi$	$\|\rho_1\| = 1$, $\|\rho_2\| = 0.9967$, $\|\rho_3\| = 0.9967$, $\|\rho_4\| = 1.0127$, $\|\rho_5\| = 1.0127$, $\|\rho_6\| = 0.9966$

From Table 2 we see that if using the parameters of the manipulator given in Table 1, the manipulator must work in the parametric resonance region. To avoid parametric resonance, we must adjust the parameters of the manipulator so that the manipulator works in the non-resonant region.

3.2. The PD controller

PD controller $\Delta\boldsymbol{\tau}_a$ applied on the drive links of manipulator can be selected according to the following expression

$$\Delta\boldsymbol{\tau}_a = -\mathbf{K}_D \left(\dot{\mathbf{q}}_a - \dot{\mathbf{q}}_a^R \right) - \mathbf{K}_P \left(\mathbf{q}_a - \mathbf{q}_a^R \right) = -\mathbf{K}_D\dot{\mathbf{y}} - \mathbf{K}_P\mathbf{y}. \tag{12}$$

The linearized equation according to Eq. (5) now takes the form

$$\mathbf{M}_L(t)\ddot{\mathbf{y}} + \mathbf{C}_L(t)\dot{\mathbf{y}} + \mathbf{K}_L(t)\mathbf{y} = \mathbf{h}_L(t) - \mathbf{K}_D\dot{\mathbf{y}} - \mathbf{K}_P\mathbf{y}. \tag{13}$$

In which $\mathbf{K}_D$ and $\mathbf{K}_P$ are diagonal matrices with positive elements as

$$\mathbf{K}_D = \begin{bmatrix} k_{d1} & 0 & 0 \\ 0 & k_{d2} & 0 \\ 0 & 0 & 0 \end{bmatrix}, \quad \mathbf{K}_P = \begin{bmatrix} k_{p1} & 0 & 0 \\ 0 & k_{p2} & 0 \\ 0 & 0 & 0 \end{bmatrix}. \tag{14}$$

From Eqs. (13) and (14) yields

$$\mathbf{M}_L^{(1)}(t)\ddot{\mathbf{y}} + \mathbf{C}_L^{(1)}(t)\dot{\mathbf{y}} + \mathbf{K}_L^{(1)}(t)\mathbf{y} = \mathbf{h}_L^{(1)}(t), \tag{15}$$

where

$$\mathbf{M}_L^{(1)}(t) = \mathbf{M}_L(t), \quad \mathbf{K}_L^{(1)}(t) = \mathbf{K}_L(t) + \mathbf{K}_P, \quad \mathbf{C}_L^{(1)}(t) = \mathbf{C}_L(t) + \mathbf{K}_D, \quad \mathbf{h}_L^{(1)}(t) = \mathbf{h}_L(t). \quad (16)$$

Eq. (15) can then be expressed in the compact form as

$$\dot{\mathbf{x}} = \mathbf{P}(t)\mathbf{x} + \mathbf{f}(t), \tag{17}$$

where we use the state variable $\mathbf{x}$

$$\mathbf{x} = \begin{bmatrix} \mathbf{y} \\ \dot{\mathbf{y}} \end{bmatrix}, \quad \dot{\mathbf{x}} = \begin{bmatrix} \dot{\mathbf{y}} \\ \ddot{\mathbf{y}} \end{bmatrix}. \tag{18}$$

The matrix of coefficients $\mathbf{P}(t)$ and vector $\mathbf{f}(t)$ are defined by

$$\mathbf{P}(t) = \begin{bmatrix} 0 & \mathbf{E} \\ -\mathbf{M}_L^{(1)^{-1}}\mathbf{K}_L^{(1)} & -\mathbf{M}_L^{(1)^{-1}}\mathbf{C}_L^{(1)} \end{bmatrix}, \quad \mathbf{f}(t) = \begin{bmatrix} 0 \\ \mathbf{M}_L^{(1)^{-1}}\mathbf{h}_L^{(1)} \end{bmatrix}. \tag{19}$$

To study the dynamic stability conditions of flexible manipulators, we need to investigate the properties of the homogeneous linear differential system that corresponds to Eq. (17)

$$\dot{\mathbf{x}} = \mathbf{P}(t)\mathbf{x}, \tag{20}$$

where $\mathbf{P}(t)$ is a continuous matrix with period T. Based on the stable criteria according to Floquet multipliers, a numerical algorithm for calculating the Floquet multipliers was presented in [23]. The gain values of the PD controller are chosen so that absolute values of Floquet multipliers are less than 1.

3.3. A procedure for determination of gain values according to Floquet multipliers using the Taguchi method

Taguchi developed the orthogonal array method to study the systems in a more convenient and rapid way, whose performance is affected by different factors when the system study becomes more complicated with the increase in the number of factors [24–28]. This method can be used to select the best results by optimization of parameters with a minimum number of test runs. We note that the Taguchi method has the following advantages: It is not necessary to use the derivative of the target function to calculate optimal parameters, and the method allows the determination of multiple stable parameters for the linear differential systems with time-periodic coefficients of complex structures.

This subsection aims to present numerical results that verify the procedure discussed above by using the Taguchi method.

Step 1: Selection of control parameters and initial levels of control parameters

The control parameters are chosen as components of two matrices of additional control torques

$$\mathbf{K}_P = \begin{bmatrix} k_{p1} & 0 & 0 \\ 0 & k_{p2} & 0 \\ 0 & 0 & 0 \end{bmatrix}, \quad \mathbf{K}_D = \begin{bmatrix} k_{d1} & 0 & 0 \\ 0 & k_{d2} & 0 \\ 0 & 0 & 0 \end{bmatrix}. \tag{21}$$

The gain values of PD controller are chosen as components of the vector of control parameters which has the following form

$$\mathbf{x} = \begin{bmatrix} x_1 & x_2 & x_3 & x_4 \end{bmatrix}^T = \begin{bmatrix} k_{p1} & k_{p2} & k_{d1} & k_{d2} \end{bmatrix}^T. \tag{22}$$

Three initial levels of each control parameter are given in Table 3.

Table 3. Control parameters and initial levels of each control parameter

Levels	Control parameters			
	k_{p1}	k_{p2}	k_{d1}	k_{d2}
1	0.1	0.01	0.01	0.01
2	3	0.2	5	0.1
3	10	25	30	35

Step 2: Calculation of Floquet multipliers and selection of target function

The Floquet multipliers of the differential equations (20) are calculated to the numerical algorithms in [24] and can be arranged in a vector as follows

$$\boldsymbol{\rho} = \begin{bmatrix} \rho_1 & \rho_2 & \rho_3 & \rho_4 & \rho_5 & \rho_6 \end{bmatrix}^T. \tag{23}$$

Step 3: Selection of orthogonal array and calculation of signal-to noise ratio (SNR)

Three levels of each control parameter are applied, necessitating the use of an L9 orthogonal array [24, 25]. Coding stage 1, stage 2, stage 3 of the control parameters are the symbols 1, 2, 3. The signal-to noise ratio (SNR) of the vector of control parameters x is calculated according to the following formula [24, 26]

$$\eta_j = (\text{SNR})_j = -10 \log_{10}(|\rho_{\max}|_j - \rho_d)^2, \quad j = 1, 2, \dots, 9 \tag{24}$$

where $|\rho_{\max}|_j$ is the biggest modulus of Floquet multipliers in the jth experiment, and ρ_d is the target Floquet multiplier. The desired value of the target Floquet multipliers is usually chosen empirically. In this example we choose $\rho_d = 0.4$. The obtained results are shown in the Table 4.

Table 4. Experimental design using L9 orthogonal array

Trial (j)	Control parameters				Results	
	k_{p1}	k_{p2}	k_{d1}	k_{d2}	$|\rho|_{max}$	SNR
1	1	1	1	1	0.9797	21.9716
2	1	2	2	2	0.9607	24.3338
3	1	3	3	3	0.9934	20.5969
4	2	1	2	3	0.9995	20.0417
5	2	2	3	1	0.8180	21.7272
6	2	3	1	2	0.9798	21.9636
7	3	1	3	2	0.8405	24.5169
8	3	2	1	3	0.9887	21.0389
9	3	3	2	1	0.9473	26.4990

Step 4: Analysis of signal-to-noise ratio

From the values of SNR of control parameters in the Table 4 we can calculate the mean value of the SNR of control parameters corresponds to the levels 1, 2, 3

$$\text{SNR}\left(k_{p1}^1\right) = [\text{SNR}(1) + \text{SNR}(2) + \text{SNR}(3)]/3 = 22.30077,$$

$$\text{SNR}\left(k_{p1}^2\right) = [\text{SNR}(4) + \text{SNR}(5) + \text{SNR}(6)]/3 = 21.24417,$$

$$\text{SNR}\left(k_{p1}^3\right) = [\text{SNR}(7) + \text{SNR}(8) + \text{SNR}(9)]/3 = 24.01827,$$

$$\text{SNR}\left(k_{p2}^1\right) = [\text{SNR}(1) + \text{SNR}(4) + \text{SNR}(7)]/3 = 22.17673,$$

$$\text{SNR}\left(k_{p2}^2\right) = [\text{SNR}(2) + \text{SNR}(5) + \text{SNR}(8)]/3 = 22.36663,$$

$$\text{SNR}\left(k_{p2}^3\right) = [\text{SNR}(3) + \text{SNR}(6) + \text{SNR}(9)]/3 = 23.01983,$$

$$\text{SNR}\left(k_{d1}^1\right) = [\text{SNR}(1) + \text{SNR}(6) + \text{SNR}(8)]/3 = 21.65803,$$

$$\text{SNR}(k_{d1}^2) = [\text{SNR}(2) + \text{SNR}(4) + \text{SNR}(9)]/3 = 23.62483,$$

$$\text{SNR}(k_{d1}^3) = [\text{SNR}(3) + \text{SNR}(5) + \text{SN }R(7)]/3 = 22.28033,$$

$$\text{SNR}\left(k_{d2}^1\right) = [\text{SNR}(1) + \text{SNR}(5) + \text{SNR}(9)]/3 = 23.39927,$$

$$\text{SNR}(k_{d2}^2) = [\text{SNR}(2) + \text{SNR}(6) + \text{SNR}(7)]/3 = 23.60477,$$

$$\text{SNR}(k_{d2}^3) = [\text{SNR}(3) + \text{SNR}(4) + \text{SNR}(8)]/3 = 20.55917,$$

in which SNR $\left(k_{p1}^1\right)$, SNR $\left(k_{p1}^2\right)$, SNR $\left(k_{p1}^3\right)$, SNR $\left(k_{d1}^1\right)$, SNR (k_{d1}^2), SNR (k_{d1}^3), SNR $\left(k_{p2}^1\right)$, SNR $\left(k_{p2}^2\right)$, SNR $\left(k_{p2}^3\right)$, SNR $\left(k_{d2}^1\right)$, SNR (k_{d2}^2), SNR (k_{d2}^3) are the mean square deviation

of the control parameters $k_{p1}^1, k_{p1}^2, k_{p1}^3, k_{d1}^1, k_{d1}^2, k_{d1}^3, k_{p2}^1, k_{p2}^2, k_{p2}^3, k_{d2}^1, k_{d2}^2, k_{d2}^3$ at the levels 1, 2, 3, respectively.
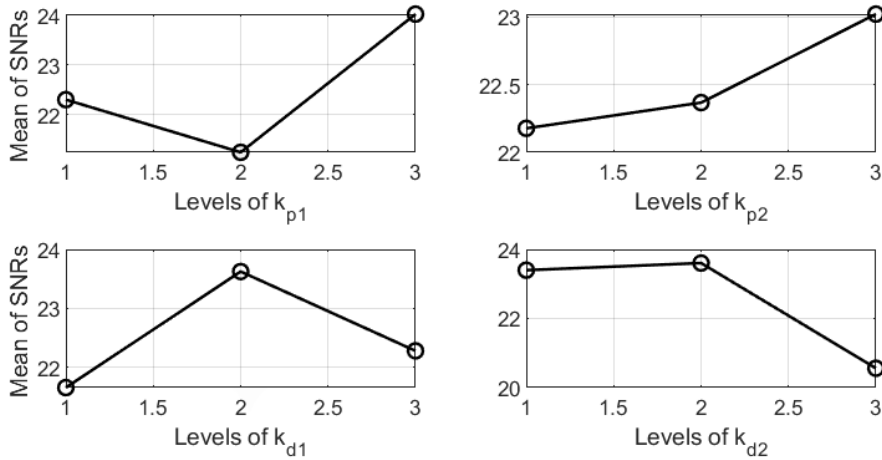

Fig. 2. Diagram of level distribution of mean signal-to-noise ratio of the control parameters

Then the signal-to noise ratio (SNR) of the control parameters can be plotted to use for optimization of seat displacement as shown in Fig. 2. From Fig. 2, the optimal signal-to-noise ratio of the control parameters can be derived as follows

$$\text{SNR}(k_{p1}) = 24.01827, \quad \text{SNR}(k_{p2}) = 23.01983, \quad \text{SNR}(k_{d1}) = 23.62483, \quad \text{SNR}(k_{d2}) = 23.60477. \quad (25)$$

Step 5: Selection of new levels for control parameters

It can be seen from Eq. (25) that the optimal values of $\text{SNR}(k_{pi})$ and $\text{SNR}(k_{di})$ perform iterative calculation. Firstly, new levels for control parameters are selected. Based on the level distribution diagram of the parameter as shown in Fig. 2, we choose the new levels of control parameters as follows: The optimal parameters are levels with the largest value of the parameters, namely, k_{p1} level 3, k_{p2} level 3, k_{d1} level 2, k_{d2} level 2. Therefore, we have the values of the new levels as follows:

If level 1 is optimal then the next levels are

New level 1   level 1   level 2   level 3

         New level 2   New level 3
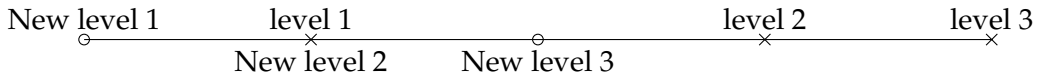
$$
\begin{cases}
\text{level 2\_new} = \text{level 1\_old} \\[2mm]
\text{level 1\_new} = \text{level 1\_old} - \dfrac{\text{level 2\_old} - \text{level 1\_old}}{2} \\[2mm]
\text{level 3\_new} = \text{level 1\_old} + \dfrac{\text{level 2\_old} - \text{level 1\_old}}{2}
\end{cases}
$$

If level 2 is optimal then the next levels are

level 1   level 2   level 3

   New level 1   New level 2   New level 3
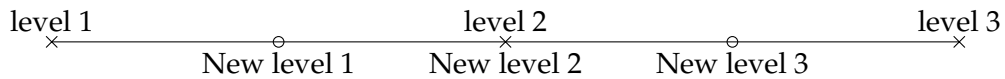
$$
\begin{cases}
\text{level 2\_new} = \text{level 2\_old} \\[2mm]
\text{level 1\_new} = \text{level 2\_old} - \dfrac{\text{level 2\_old} - \text{level 1\_old}}{2} \\[2mm]
\text{level 3\_new} = \text{level 2\_old} + \dfrac{\text{level 3\_old} - \text{level 2\_old}}{2}
\end{cases}
$$

If level 3 is optimal then the next levels are

level 1   level 2   level 3   New level 3

     New level 1   New level 2
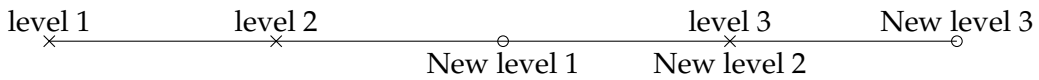
$$
\begin{cases}
\text{level 2\_new} = \text{level 3\_old} \\[2mm]
\text{level 1\_new} = \text{level 3\_old} - \dfrac{\text{level 3\_old} - \text{level 2\_old}}{2} \\[2mm]
\text{level 3\_new} = \text{level 3\_old} + \dfrac{\text{level 3\_old} - \text{level 2\_old}}{2}
\end{cases}
$$

According to the rule presented above, we have the new levels of control parameters as shown in Table 5.

Table 5. Control factors and new levels of control parameters

Levels	Control parameters			
	k_{p1}	k_{p2}	k_{d1}	k_{d2}
1	6.5	12.6	2.5	0.055
2	10	25	5	0.1
3	13.5	37.4	17.5	17.55

Then the analysis of signal-to-noise ratio (SNR) is performed as Step 2.

Step 6: Check the convergence condition of the signal-to-noise ratio (SNR) and determine the optimal control parameters

After 60 iterations, we obtain the optimal noise values of the control parameters. The calculation results are shown in Table 6.

Table 6. SNR values of the control parameters and ANOM and ANOVA in the row of the SNR

Trial	Calculation Results					
	SNR (k_{p1})	SNR (k_{p2})	SNR (k_{d1})	SNR (k_{d2})	Mean	Variance
1	5.6523	5.7342	6.4098	5.849	5.911325	0.087707237
2	14.3583	20.3713	14.634	14.4645	15.957025	6.504942857
3	22.118	20.6996	23.6227	19.0499	21.37255	2.866608863
4	30.0972	35.592	31.9126	44.4944	35.52405	30.74126709
5	38.3261	41.7656	39.2035	37.4125	39.176925	2.634760812
...	...	...	...	...	...	...
56	137.2585	137.2585	137.2585	137.2585	137.2585	0
57	137.2585	137.2585	137.2585	137.2585	137.2585	0
58	137.2585	137.2585	137.2585	137.2585	137.2585	0
59	137.2585	137.2585	137.2585	137.2585	137.2585	0
60	137.2585	137.2585	137.2585	137.2585	137.2585	0

To determine the mean and variance of SNR we use the following formulas

$$\text{Mean} = \frac{\text{SNR}(k_{p1}) + \text{SNR}(k_{p2}) + \text{SNR}(k_{d1}) + \text{SNR}(k_{d2})}{4}, \tag{26}$$

$$\text{Variance} = \frac{[\text{SNR}(k_{p1}) - \text{Mean}]^2 + [\text{SNR}(k_{p2}) - \text{Mean}]^2}{4} + \frac{[\text{SNR}(k_{d1}) - \text{Mean}]^2 + [\text{SNR}(k_{d2}) - \text{Mean}]^2}{4}. \tag{27}$$

According to the above analysis, we obtain the optimal parameters of after 60 iterations. The optimal control parameters are given as follows

$$k_{p1} = 9.0838, \quad k_{p2} = 0.1057, \quad k_{d1} = 20.478, \quad k_{d2} = 0.0026. \tag{28}$$

Using these values, it is easy to find the Floquet multipliers of Eq. (20) as follows

$$\rho_1 = 0.4000, \quad \rho_2 = 0.0607 + 0.3168i, \quad \rho_3 = 0.0607 - 0.3168i,$$
$$\rho_4 = -0.0001 + 0.0000i, \quad \rho_5 = 0, \quad \rho_6 = 0. \tag{29}$$

From Eqs. (29) yields modulus of Floquet multipliers

$$|\rho_1| = 0.4, \quad |\rho_2| = 0.3226, \quad |\rho_3| = 0.3226, \quad |\rho_4| = 0.0001, \quad |\rho_5| = 0, \quad |\rho_6| = 0. \quad (30)$$

3.4. Determine control parameters in a number of common speed ranges

We choose the desired motion rule of the active links in the following form

$$q_{a1} = 0.025\cos(\Omega t), \quad q_{a2} = \pi/4\cos(\Omega t). \tag{31}$$

Using the algorithm presented in paragraph 3.3, we can determine the control parameters corresponding to some popular speed ranges as follows Table 7.

Table 7. Control parameters in several speed ranges

Ω	ρ_d	k_{p1}	k_{p2}	k_{d1}	k_{d2}
π	0.4	9.0838	0.1057	20.478	0.0026
2π	0.4	14.8229	0.1296	17.5	0.065
4π	0.5	11.7505	0.0764	6.1743	0.064
8π	0.75	7.3226	0.1064	8.0228	0.0604
9π	0.9	13.8598	0.0507	28.4096	0.0525

The transition oscillation of the system depends on the initial conditions. For illustration, we assume that the initial conditions are chosen as follows

$$t = 0 : \mathbf{x}(0) = \begin{bmatrix} 0 & 0 & 0.25\pi & 0.25\pi^2 \end{bmatrix}^T. \tag{32}$$

We calculate transient vibration of the flexible manipulator with the parameters given in Table 7. Some calculation results of the transient vibration are shown in Figs. 3, 4, 5 and 6.
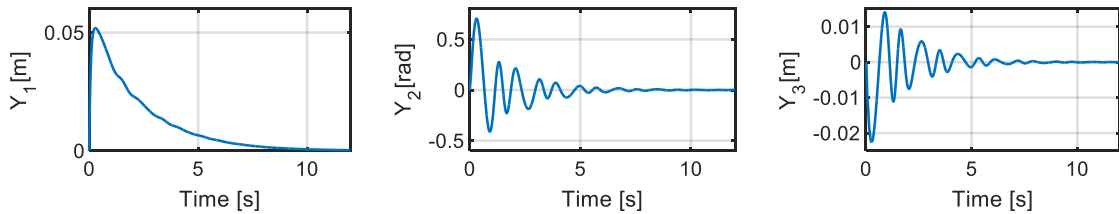
Fig. 3. Transient vibration of the flexible manipulator with control torque case $\Omega = \pi\,(\text{rad}/\text{s})$

From Figs. 3–6, we can see that with the selected control parameter, the transient vibration of the flexible manipulator decreases to zero relatively quickly. In other words, the dynamic stability of the flexible manipulator is guaranteed by a simple PD controller.
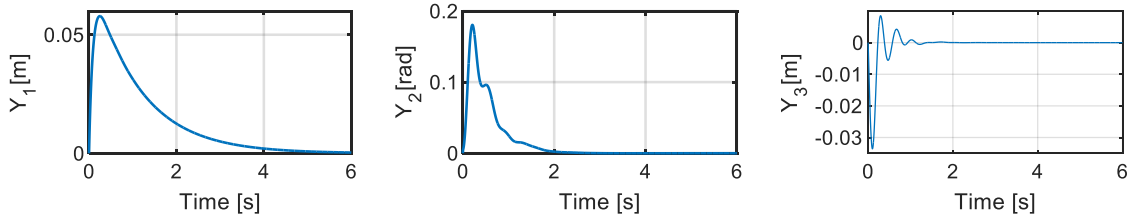
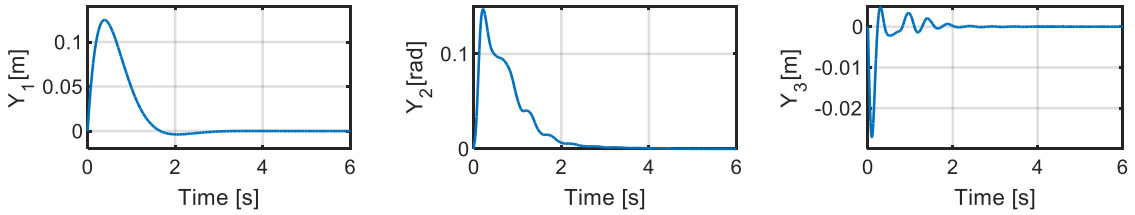*Fig. 4.* Transient vibration of the flexible manipulator with control torque case $\Omega = 2\pi \, (\text{rad/s})$

Fig. 5. Transient vibration of the flexible manipulator with control torque case $\Omega = 4\pi \, (\text{rad/s})$
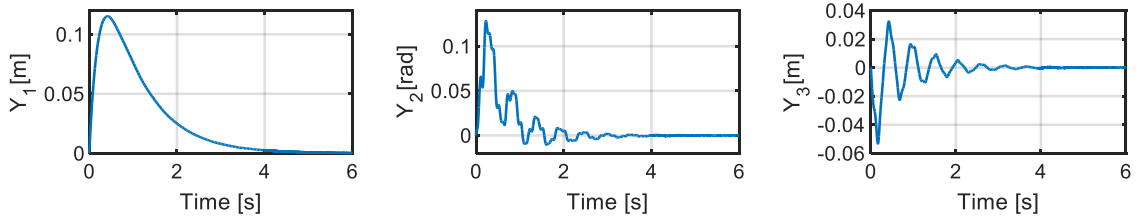

Fig. 6. Transient vibration of the flexible manipulator with control torque case $\Omega = 8\pi \, (\text{rad/s})$

4. CALCULATION OF PERIODIC VIBRATION OF A FLEXIBLE MANIPULATOR

The linearized differential equations of motion of the two-link rigid-flexible manipulator have the following form

$$\mathbf{M}_L^{(1)}(t)\ddot{\mathbf{y}} + \mathbf{C}_L^{(1)}(t)\dot{\mathbf{y}} + \mathbf{K}_L^{(1)}(t)\mathbf{y} = \mathbf{h}_L^{(1)}(t). \tag{33}$$

As known in the theory of linear differential equations [16, 17] when the system of homogeneous linear differential equations is asymptotically stable, then the system of differential equations having the right side (33) has periodic solution. Using the algorithm proposed by Khang et al. [23], the periodic oscillation of the system of equations (33) can be calculated in the following form

$$\mathbf{y}^* = \begin{bmatrix} \mathbf{y}_1^* & \mathbf{y}_2^* \end{bmatrix}. \tag{34}$$

When the parameters $\mathbf{K}_P$ and $\mathbf{K}_D$ are chosen so that the system of homogeneous linear differential equations is asymptotically stable is stable quickly, the solution of equation (33) has the form

$$\mathbf{y} \approx \mathbf{y}^*. \tag{35}$$

Using the control parameters in Table 7, some simulation results of solutions of Eq. (23) are shown in Figs. 7–9.
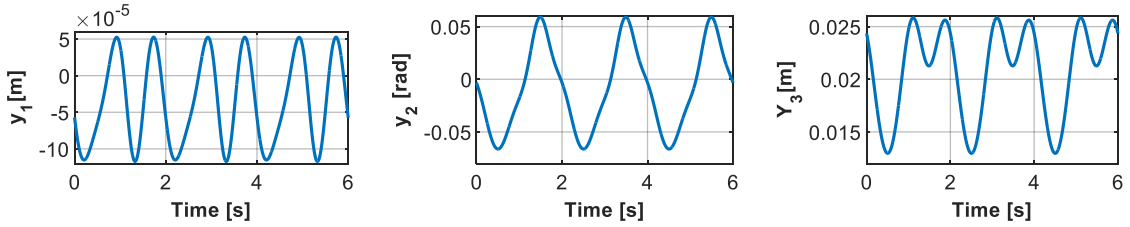

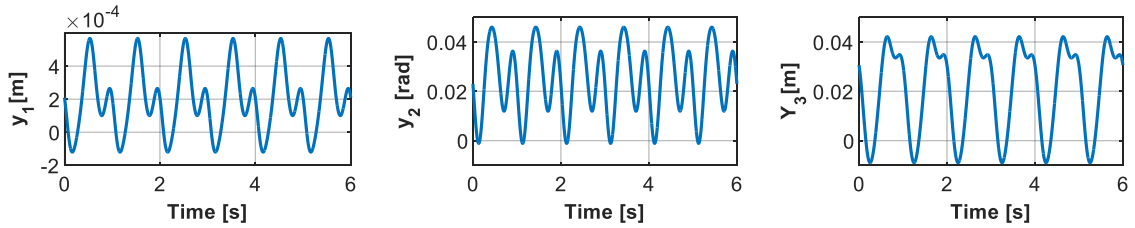*Fig. 7.* Periodic vibrations of perturbed motions by $\Omega = \pi(\text{rad}/\text{s})$

Fig. 8. Periodic vibrations of perturbed motions by $\Omega = 2\pi(\text{rad}/\text{s})$
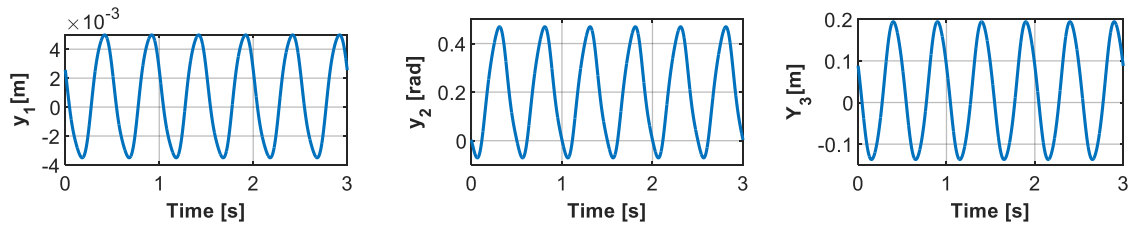
Fig. 9. Periodic vibrations of perturbed motions by $\Omega = 4\pi(\text{rad}/\text{s})$

From perturbed motions y, we call determine the generalized coordinates, velocities and accelerations of the flexible manipulator

$$q_{ai}(t) \approx q_{ai}^R(t) + y_i(t), \ i = 1, \ldots, n; \quad q_{ej}(t) = y_{n+j} \ (j = 1, \ldots, m). \tag{36}$$

5. CALCULATION OF INVERSE DYNAMICS OF THE FLEXIBLE MANIPULATOR BASED ON THE LINEARIZATION

In previous sections, the stability analysis, and the calculation of periodic vibration of the flexible manipulator have been studied. In this section an approximate approach for calculation of inverse dynamics of flexible manipulator is proposed.

5.1. Determining the motion of the operating point E

From the periodic oscillation calculated above, we can find the elastic displacement of the elastic beam DE

$$w(x, t) = X_1(x)y_3(t). \tag{37}$$

From Eq. (37) we have the elastic displacement from point E

$$w(l_2, t) = X_1(l_2)y_3(t). \tag{38}$$

Then the position of the point E on the elastic link is given as

$$x_E(t) = l_1 + (r + l_2)\cos(q_{a2}^R + y_2) - w(l_2, t)\sin(q_{a2}^R + y_2), \tag{39}$$

$$y_E(t) = q_{a1}^R + y_1 + (r + l_2)\sin(q_{a2}^R + y_2) + w(l_2, t)\cos(q_{a2}^R + y_2). \tag{40}$$

Using the control parameters in Table 7, some simulation results of the position of point E are shown in Figs. 10–12. In Figs. 10–12, the solid lines represent the motion graph of operation point E when the DE link is an elastic beam, the dashed lines represent the motion graph of operation point E when the DE link is a rigid link.
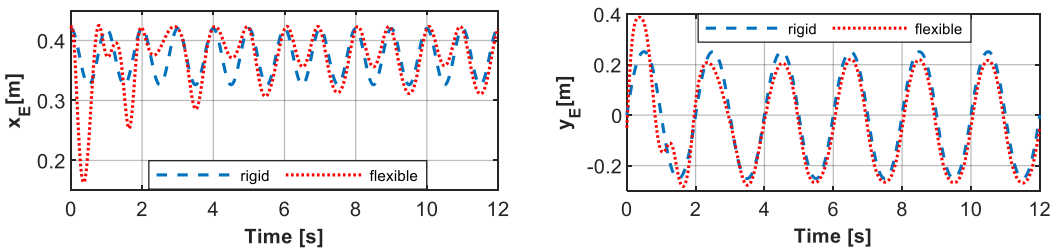

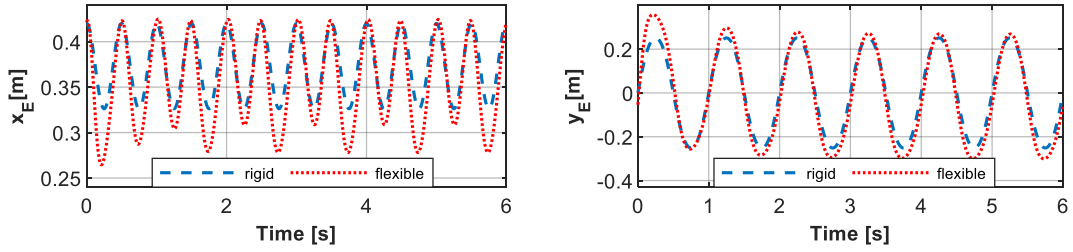*Fig. 10.* Motion graph of operating point E by $\Omega = \pi(\text{rad}/\text{s})$

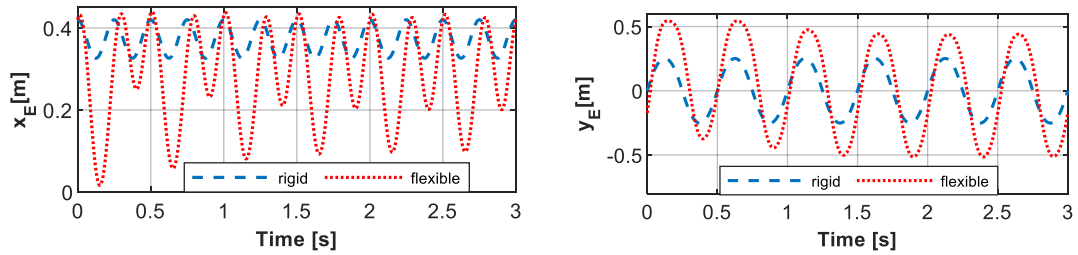Fig. 11. Motion graph of operating point E by $\Omega = 2\pi(\mathrm{rad/s})$

Fig. 12. Motion graph of operating point E by $\Omega = 4\pi(\mathrm{rad/s})$

5.2. Calculating inverse dynamics of flexible manipulator

Substitution of Eqs. (36)–(40) in differential equations of the manipulator T-R, we can obtain the actuator torques of the two-link rigid-flexible manipulator [20]

$$
F = F_{d1} + (m_1 + m_2 + m_B)\ddot{q}_{a1} + [(\frac{1}{2}m_2l_2 + m_2r)\cos q_{a2} - \mu C_1 q_{e2} \sin q_{a2}]\ddot{q}_{a2} + \mu \cos q_{a2}C_1\ddot{q}_{e1}
$$
$$
- (\frac{1}{2}m_2l_2 + m_2r)\dot{q}_{a2}^2 \sin q_{a2} - 2C_1\mu\dot{q}_{a2}\dot{q}_{e1}\sin q_{a2} - \mu\dot{q}_{a2}^2 C_1 q_{e1}\cos q_{a2} + (m_1 + m_2 + m_B)g,
$$
(41)

$$
\tau = [(\frac{1}{2}m_2l_2 + m_2r)\cos q_{a2} - \mu C_1 q_{e1}\sin q_{a2}]\ddot{q}_{a1} + (J_B + m_2r^2 + m_2rl_2 + \frac{m_2l_2^2}{3} + \mu n_{11}q_{e1}^2)\ddot{q}_{a2}
$$
$$
+ (\mu rC_1 + \mu D_1)\ddot{q}_{e1} + 2\mu n_{11}\dot{q}_{a2}\dot{q}_{e1}q_{e1} + m_2g(r + \frac{l_2}{2})\cos q_{a2} - \mu g \sin q_{a2}C_1 q_{e1} + \tau_{d2}.
$$
(42)

The elements $F_{a1}^R(t)$, $\tau_{a2}^R(t)$ are given in reference [20]. Using the control parameters in Table 7, some calculation results of actuator torque are shown in Figs. 13–15.

In Figs. 13–15, the solid lines represent the joint torques when the DE link is an elastic beam, the dashed lines are the joint torques when the DE link is a rigid link. Through the graphs, we can see that when the angular velocity of the joint links is larger, the graph of the joint torques with elastic DE link is further away from the joint torque graph with solid link.
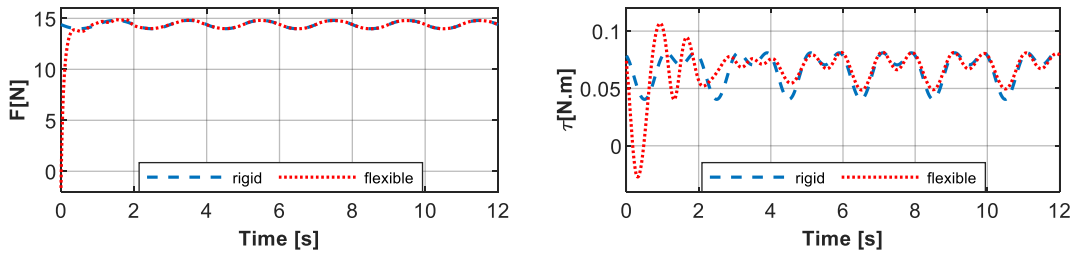
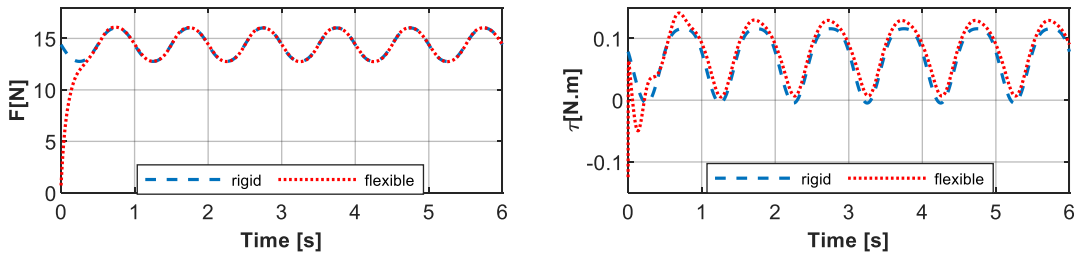*Fig. 13.* Actuator torque by $\Omega = \pi(\text{rad/s})$

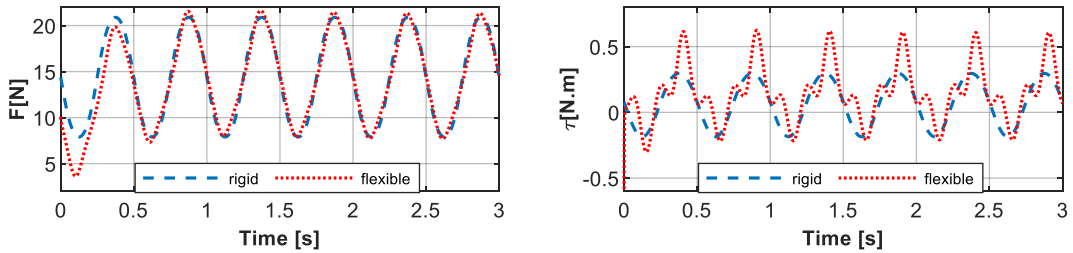*Fig. 14.* Actuator torque by $\Omega = 2\pi(\text{rad/s})$

Fig. 15. Actuator torque by $\Omega = 4\pi(\text{rad/s})$

6. CONCLUSIONS

In the present paper, the linearization problem of the equation of motion of flexible manipulator T-R in the vicinity of a fundamental motion is addressed. Then an approach for the computation of dynamic stability control and the inverse dynamics of flexible manipulators has been presented.

A procedure for the optimal design of control parameters of the homogeneous linear differential equations having time-periodic coefficients is presented. In case the system is unstable, a PD controller is added to stabilize the system. Then the optimal parameters of the PD controller are found by Taguchi method. The proposed approach has been successfully applied to a flexible manipulator T-R. On the basis of the calculation of the

oscillation of the flexible manipulator, an algorithm for finding the actuator torques of the flexible manipulator T-R has been implemented.

Through numerical simulation, the efficiency and usefulness of the proposed algorithm were demonstrated. The algorithm presented in this paper can be applied to calculate dynamic stability control and the inverse dynamics of flexible manipulators with many elastic links.

ACKNOWLEDGEMENT

REFERENCES

[1] A. A. Shabana. Flexible multibody dynamics: Review of past and recent development. *Multibody System Dynamics*, **1**, (2), (1997), pp. 189–222. https://doi.org/10.1023/a:1009773505418.

[2] S. K. Dwivedy and P. Eberhard. Dynamic analysis of flexible manipulators, a literature review. *Mechanism and Machine Theory*, **41**, (2006), pp. 749–777. https://doi.org/10.1016/j.mechmachtheory.2006.01.014.

[3] H. N. Rahimi and M. Nazemizadeh. Dynamic analysis and intelligent control techniques for flexible manipulators: a review. *Advanced Robotics*, **28**, (2013), pp. 63–76. https://doi.org/10.1080/01691864.2013.839079.

[4] K. Lochan, B. K. Roy, and B. Subudhi. A review on two-link flexible manipulators. *Annual Reviews in Control*, **42**, (2016), pp. 346–367. https://doi.org/10.1016/j.arcontrol.2016.09.019.

[5] B. C. Chiou and M. Shahinpoor. Dynamic stability analysis of a two-link force-controlled flexible manipulator. *Journal of Dynamic Systems, Measurement, and Control*, **112**, (1990), pp. 661–666. https://doi.org/10.1115/1.2896192.

[6] A. S. Yigit. On the stability of PD control for a two-link rigid-flexible manipulator. *Journal of Dynamic Systems, Measurement, and Control*, **116**, (1994), pp. 208–215. https://doi.org/10.1115/1.2899212.

[7] N. Popplewell and D. Chang. Influence of an offset payload on a flexible manipulator. *Journal of Sound and Vibration*, **190**, (1996), pp. 721–725. https://doi.org/10.1006/jsvi.1996.0087.

[8] S. Choura and A. S. Yigit. Control of a two-link rigid-flexible manipulator with a moving payload mass. *Journal of Sound and Vibration*, **243**, (2001), pp. 883–897. https://doi.org/10.1006/jsvi.2000.3449.

[9] A. A. Ata, W. F. Fares, and M. Y. Saadeh. Dynamic analysis of a two-link flexible manipulator subject to different sets of conditions. *Procedia Engineering*, **41**, (2012), pp. 1253–1260. https://doi.org/10.1016/j.proeng.2012.07.308.

[10] X. Yang, S. S. Ge, and W. He. Dynamic modelling and adaptive robust tracking control of a space robot with two-link flexible manipulators under unknown disturbances. *International Journal of Control*, **91**, (2017), pp. 969–988. https://doi.org/10.1080/00207179.2017.1300837.

[11] P. Kumar and B. Pratiher. Modal characterization with nonlinear behaviors of a two-link flexible manipulator. *Archive of Applied Mechanics*, **89**, (2019), pp. 1201–1220. https://doi.org/10.1007/s00419-018-1472-9.

[12] H. Asada, Z.-D. Ma, and H. Tokumaru. Inverse dynamics of flexible robot arms: modeling and computation for trajectory control. *Journal of Dynamic Systems, Measurement, and Control*, **112**, (1990), pp. 177–185. https://doi.org/10.1115/1.2896124.

[13] E. Bayo and H. Moulin. An efficient computation of the inverse dynamics of flexible manipulators in the time domain. In *IEEE International Conference on Robotics and Automation*, IEEE Computer Society, IEEE Computer Society, (1989), pp. 710–711.

[14] E. Bayo, P. Papadopoulos, J. Stubbe, and M. A. Serna. Inverse dynamics and kinematics of multi-link elastic robots: an iterative frequency domain approach. *The International Journal of Robotics Research*, **8**, (1989), pp. 49–62. https://doi.org/10.1177/027836498900800604.

[15] J. G. De Jalon and E. Bayo. *Kinematic and dynamic simulation of multibody systems: the real-time challenge*. Springer, Berlin, (1994).

[16] J. K. Hale. *Oscillations in nonlinear systems*. McGraw-Hill, New York, (1963).

[17] B. P. Demidovich. *Lectures on the Mathematical Stability Theory*. Nauka, Moscow, (1967). (in Rusian).

[18] W. Schiehlen and P. Eberhard. *Applied dynamics*. Springer International Publishing Switzerland, (2014).

[19] S. Briot and W. Khalil. *Dynamics of parallel robot, from rigid bodies to flexible elements*. Springer, Switzerland, (2015).

[20] D. C. Dat, N. V. Khang, and N. T. V. Huong. Linearization of the motion equations of flexible robot manipulators. In *Proceedings of the 2th National Conference on Dynamics and Control, Bach Khoa Publishing House, Hanoi*, (2022).

[21] N. V. Khang, N. P. Dien, and H. M. Cuong. Linearization and parametric vibration analysis of some applied problems in multibody systems. *Multibody System Dynamics*, **22**, (2009), pp. 163–180. https://doi.org/10.1007/s11044-009-9156-4.

[22] N. V. Khang, N. S. Nam, and N. V. Quyen. Symbolic linearization and vibration analysis of constrained multibody systems. *Archive of Applied Mechanics*, **88**, (2018), pp. 1369–1384. https://doi.org/10.1007/s00419-018-1376-8.

[23] N. V. Khang and N. P. Dien. Parametric vibration analysis of transmission mechanisms using numerical methods. *Advances in Vibration Engineering and Structural Dynamics, Edited by FB Carbajal, Intech, Croatia*, (2012), pp. 301–331.

[24] G. Taguchi, S. Chowdhury, and Y. Wu. *Taguchi's quality engineering handbook*. John Wiley & Sons, New Jersey, (2005).

[25] R. A. Zambanini. The application of Taguchi's method of parameter design to the design of mechanical systems. Master's thesis, Lehigh University, (1992).

[26] R. K. Roy. *Design of experiments using the Taguchi approach*. John Wiley and Sons, New York, (2001).

[27] N. V. Khang, V. D. Phuc, N. T. V. Huong, and D. T. Duong. Optimal control of transverse vibration of Euler-Bernoulli beam with multiple dynamic vibration absorbers using Taguchi's method. *Vietnam Journal of Mechanics*, **40**, (2018), pp. 265–283. https://doi.org/10.15625/0866-7136/11366.

[28] N. V. Khang, D. T. Duong, N. T. V. Huong, N. D. T. T. Dinh, and V. D. Phuc. Optimal control of vibration by multiple tuned liquid dampers using Taguchi method. *Journal of Mechanical Science and Technology*, **33**, (2019), pp. 1563–1572. https://doi.org/10.1007/s12206-019-0308-z.